Astronomy & Astrophysics

The VIMOS VLT Deep Survey[*]

Tracing the galaxy stellar mass assembly history over the last 8 Gyr

D. Vergani[1],[**], M. Scodeggio[1], L. Pozzetti[2], A. Iovino[3], P. Franzetti[1], B. Garilli[1], G. Zamorani[2], D. Maccagni[1], F. Lamareille[2], O. Le Fèvre[4], S. Charlot[5,6], T. Contini[7], L. Guzzo[3], D. Bottini[1], V. Le Brun[4], J. P. Picat[7], R. Scaramella[8,9], L. Tresse[4], G. Vettolani[8], A. Zanichelli[8], C. Adami[4], S. Arnouts[4], S. Bardelli[2], M. Bolzonella[2], A. Cappi[2], P. Ciliegi[2], S. Foucaud[10], I. Gavignaud[11], O. Ilbert[12], H. J. McCracken[6,13], B. Marano[14], C. Marinoni[15], A. Mazure[4], B. Meneux[1,2], R. Merighi[2], S. Paltani[16,17], R. Pellò[7], A. Pollo[4,18], M. Radovich[19], E. Zucca[2], M. Bondi[8], A. Bongiorno[14], J. Brinchmann[20], O. Cucciati[3,21], S. de la Torre[4], L. Gregorini[8,14], E. Perez-Montero[7], Y. Mellier[6,13], P. Merluzzi[19], and S. Temporin[22]

(Affiliations can be found after the references)

ABSTRACT

Aims. Our aim is to investigate the history of mass assembly for galaxies of different stellar masses and types.

Methods. We selected a mass-limited sample of 4048 objects from the VIMOS VLT Deep Survey (VVDS) in the redshift interval $0.5 \leq z \leq 1.3$. We then used an empirical criterion, based on the amplitude of the 4000 Å Balmer break ($D_n 4000$), to separate the galaxy population into spectroscopically early- and late-type systems. The equivalent width of the [OII]3727 line is used as proxy for the star formation activity. We also derived a type-dependent stellar mass function in three redshift bins.

Results. We discuss to what extent stellar mass drives galaxy evolution, showing for the first time the interplay between stellar ages and stellar masses over the past 8 Gyr. Low-mass galaxies have small $D_n 4000$ and at increasing stellar mass, the galaxy distribution moves to higher $D_n 4000$ values as observed in the local Universe. As cosmic time goes by, we witness an increasing abundance of massive spectroscopically early-type systems at the expense of the late-type systems. This spectral transformation of late-type systems into old massive galaxies at lower redshift is a process started at early epochs ($z > 1.3$) and continuing efficiently down to the local Universe. This is also confirmed by the evolution of our type-dependent stellar mass function. The underlying stellar ages of late-type galaxies apparently do not show evolution, most likely as a result of a continuous and efficient formation of new stars. All star formation activity indicators consistently point towards a star formation history peaked in the past for massive galaxies, with little or no residual star formation taking place in the most recent epochs. In contrast, most of the low-mass systems show just the opposite characteristics, with significant star formation present at all epochs. The activity and efficiency of forming stars are mechanisms that depend on galaxy stellar mass, and the stellar mass assembly becomes progressively less efficient in massive systems as time elapses. The concepts of star formation downsizing and mass assembly downsizing describe a single scenario that has a top-down evolutionary pattern in how the star formation is quenched, as well as how the stellar mass is grown. The role of (dry) merging events seems to be only marginal at $z < 1.3$, as our estimated efficiency in stellar mass assembly can possibly account for the progressive accumulation of observed passively evolving galaxies.

Key words. galaxies: formation – galaxies: evolution – galaxies: fundamental parameters – galaxies: luminosity function, mass function – cosmology: observations

1. Introduction

How galaxies form and evolve with cosmic time is one of the key questions in observational cosmology. A fundamental role towards answering this question is played by deep surveys sampling over a thousand galaxies on large portions of the sky. The global star formation history is reasonably well known out to very high redshifts and with considerable details up to $z \sim 1$ (see for a recent summary Hopkins & Beacom 2006), but the role of the various physical mechanisms contributing to the assembly of galaxy stellar mass is still unclear, as is their importance at different epochs.

In agreement with the first formulation introduced by Cowie et al. (1996), a downsizing scenario for galaxy formation persistently emerges in several observational studies (Brinchmann & Ellis 2000; Gavazzi et al. 2002; Kodama et al. 2004; Bauer et al. 2005; Feulner et al. 2005a,b; Juneau et al. 2005; Bundy et al. 2006; Borch et al. 2006; Cimatti et al. 2006; Cucciati et al. 2006; Pozzetti et al. 2007). However, observed galactic-scale properties like the quenching of star formation activity in massive galaxies not yet have been reproduced well within the ΛCDM framework (e.g. De Lucia et al. 2006; Bower et al. 2006) that successfully describes the hierarchical growth of dark matter halos and the galaxy clustering properties.

The observed discrepancies between models and observations are probably due to our limited ability to reproduce the

---

actual physics on galactic scales with simple recipes. Perhaps some feedback mechanisms are still missing in models. Thus, a phenomenological approach to the problem of the stellar mass assembly as a function of cosmic time, i.e. one that relies as much as possible on observational data, can suggest new implementations in current semi-analytical models.

In this paper we use the first epoch observations of the VIMOS-VLT Deep Survey (VVDS, Le Fèvre et al. 2005) to derive stellar masses, stellar ages and star formation efficiency for a statistically significant sample of galaxies. We analyse how stellar mass is assembled in active and quiescent galaxies classified following a spectroscopic scheme, and how this process evolves with cosmic time using spectroscopic diagnostics. This analysis provides constraints on the hierarchical scenario thought to govern dark matter assembly and can be pursued using VVDS data starting from a time when the Universe had ~30% of its present age.

The present work is organised as follows: the data and sample selection are presented in Sect. 2; the methodology we adopted to perform our analysis is described in Sect. 3. Results are given in Sect. 4 and a summary in Sects. 5. Throughout this work we assume a standard cosmological model with $\Omega_M = 0.3$, $\Omega_\Lambda = 0.7$ and $H_0 = 70 \, \mathrm{km \, s^{-1} \, Mpc^{-1}}$. Magnitudes are given in the AB system.

2. The first epoch VVDS sample

The primary observational goal of the VVDS as well as the survey strategy are presented in detail in Le Fèvre et al. (2005). Here we stress that in order to minimise possible selection biases, the VVDS has been conceived as a purely flux-limited survey, i.e. no target pre-selection according to colours or compactness is implemented. In this paper we consider the deep spectroscopic sample of the first epoch data in the VVDS-0226-04 field (from now on simply VVDS-F02) that targets objects in the magnitude range $17.5 \leq I_{AB} \leq 24$.

First-epoch spectroscopic observations in the VVDS-F02 field were carried out with the VIMOS multi-object spectrograph (Le Fèvre et al. 2005). The LRred grism was used with 1″ wide slits to cover the spectral range 5500 Å $< \lambda <$ 9400 Å with an effective spectral resolution $R \sim 230$ at $\lambda = 7500$ Å. The spectroscopic targets were selected from the photometric catalogues using the VLT-VIMOS Mask Preparation Software (VVMPS; Bottini et al. 2005). The spectroscopic multi-object exposures were reduced using the VIPGI tool (Scodeggio et al. 2005; Zanichelli et al. 2005). Further details on observations and data reduction are given in Le Fèvre et al. (2004a,b).

The first-epoch data sample in the VVDS-F02 field extends over a sky area of $0.7 \times 0.7 \, \mathrm{deg}^2$ and has a median redshift of $z \sim 0.76$. It contains 7267 objects with secure redshifts, corresponding to an average random sampling rate of 23% of the initial photometric sample. It is important to stress that we explored the VVDS-F02 redshift success rate for different galaxy types (from star-forming to quiescent galaxies) in Franzetti et al. (2007) obtaining a similar fraction of galaxy types in the photometric sample and in the spectroscopic sample. Thus we have no significant bias against special types of galaxies in our survey as our ability to obtain redshifts for star-forming and quiescent galaxies are similar.

In this work we used the [OII]λ3727 line and the 4000 Å break as indicators of star formation activity and stellar ages respectively. As a consequence, we limited our sample to galaxies within the $0.5 \leq z \leq 1.3$ redshift interval, giving us a final

number of 4277 galaxies, after removing spectroscopically confirmed broad line AGNs and stars.

This sample provides an excellent laboratory to analyse spectral properties of galaxies at several redshift ranges, especially as it is accompanied by a wealth of photometric ancillary data, collected at several telescopes and described in the following papers: McCracken et al. (*BVRI* bands at CFHT, 2003); Radovich et al. (*U*-band at ESO-2.2 m/WFI, 2004); *ubvrz* bands by the CFHT Legacy Survey project (McCracken et al. 2007), and *J* and K_s at ESO-NTT/SOFI (Iovino et al. 2005; Temporin et al. 2006).

3. Methodology

In this section we will describe in some details the methodology adopted to obtain measurements of [OII]λ3727 and D_n4000 from VVDS spectra and to derive estimates for specific star formation rates (SSFRs) and stellar masses.

3.1. Spectral measurements: [OII] and D_n4000

Spectral features measurements have been obtained for all galaxies in our sample using the *platefit_vvds* software package. This software implements the spectral feature measurement techniques described by Tremonti et al. (2004), but takes into account the lower spectral resolution of our data. Here we give a brief outline of the fitting procedure and we refer to Lamareille et al. (2007) for further details. As a first step, the best fitting stellar continuum derived from a grid of stellar population synthesis models (Bruzual & Charlot 2003, hereafter BC03) is subtracted from the observed spectrum. Any remaining residual is removed by fitting a low-order polynomial to the continuum-subtracted spectrum, and then all emission lines are fitted simultaneously with a Gaussian profile. Finally, absorption features and spectral breaks are measured after having subtracted emission-lines from the original spectrum.

The two spectral measurements we use in this paper are the equivalent width of the [OII]λ3727 doublet (*EW*[OII] from now onwards) and the amplitude of the 4000 Å break. In particular, we adopt the so-called narrow definition for the 4000 Å break (hereafter D_n4000), introduced by Balogh et al. (1999) and based on the ratio of the average spectral flux density in the bands 4050−4250 Å and 3750−3950 Å around the break. Compared to the original definition introduced by Bruzual (1983) the newly proposed index has the advantage of reducing the effect of dust reddening, because of the narrower portion of galaxy spectrum involved in the measurement (see for details Kauffmann et al. 2003a).

Comparing repeated observations available for 140 objects in our sample, we estimated that the typical relative uncertainty affecting our measurements is ~27% and ~10% for the *EW*[OII] and D_n4000, respectively. Given the typical signal-to-noise ratio of the spectra, we estimate an average detection threshold for the [OII] doublet of 8 Å. Since the D_n4000 accuracy can depend on galaxy redshift because some fringing residuals contribute to increase the noise in the VVDS spectra, we compared the repeated D_n4000 measurements separately for galaxies with $z < 0.9$ (where the measurement is not affected by fringing) and for galaxies with $z > 0.9$ (where our measurements begin to be affected by fringing). The scatter of the D_n4000 values in the two redshift bins is always within the quoted values. Therefore we can safely conclude that fringing does not significantly affect our results.

3.2. Spectral classification

To study the role played by the stellar mass in regulating the active phase of star formation, we adopt a parametric classification of galaxies based on the D_n4000 index used as an estimator of stellar ages (Hamilton 1985; Balogh et al. 1999).

We choose a value of $D_n4000 = 1.5$ to distinguish between *spectroscopic late-type* ($D_n4000 < 1.5$) and *spectroscopic early-type* ($D_n4000 > 1.5$) galaxies.

Our choice is motivated both by galaxy evolution models and observations. Single stellar population (SSP) models have shown that in a galaxy with solar metallicity experiencing an instantaneous burst of star formation, the spectrum of the underlying stellar population reaches values of D_n4000 larger than 1.5 in ~1 Gyr (Kauffmann et al. 2003a). Different results obtained using different stellar libraries are within the error of the D_n4000 measure (Kauffmann et al. 2003a; Le Borgne et al. 2006), while there is a possible dependency on metallicity for old stellar ages (>1 Gyr). Galaxies with values of metallicity as extreme as 0.05 (2.5) $Z_\odot$ reach values of D_n4000 larger than 1.5 in 2.5 (0.8) Gyr after a burst (Kauffmann et al. 2003a). Le Borgne et al. (2006) investigate the D_n4000 evolution using other modes of star formation history. They show that the D_n4000 index reaches values larger than 1.5 after 1 Gyr from the initial activity also in galaxies with a period of constant star formation truncated 0.5 Gyr after their formation, while galaxies with recurring burst modes always keep the D_n4000 values below 1.5 in a period as long as 9 Gyr.

Observationally in the present-day galaxies, values of D_n4000 smaller (larger) than 1.5 have identified young (old) stellar populations with a separation between the two populations at 1 Gyr (Kauffmann et al. 2003b). This limit has been widely used in other observational studies (Miller & Owen 2002; Mignoli et al. 2005).

We conclude that the D_n4000, despite the uncertainties discussed above, is still completely adequate to provide a broad separation of the galaxy population into active and quiescent galaxies, although it might not provide a very precise age estimate for the stellar population.

Hereafter we refer to our *spectroscopic early-* and *spectroscopic late-type* galaxies simply as early- and late-type galaxies, although the classification of a galaxy on colour, morphological, spectroscopic based schemes should be kept distinct. The different terminologies should not be mixed up, despite the robust trends existing among morphologies, colours, gas content, star formation activity, and other properties (for a recent review see Renzini 2006). The category of early-type galaxies, by virtue of their relatively simple star formation history, are generally used as the preferential category of objects to test galaxy formation and evolution and therefore one should be careful in the definition chosen to select them (see Franzetti et al. 2007).

3.3. Star formation rate estimates

Adopting the formula proposed by Guzman et al. (1997) we can translate the EW[OII] in star formation rate estimates:

$$SFR(M_\odot \text{ yr}^{-1}) \approx 10^{-11.6-0.4(M_B-M_{B_\odot})}EW[\text{OII}], \quad (1)$$

where we used the absolute magnitudes M_B as estimated in Ilbert et al. (2005). Although the average accuracy of the absolute spectrophotometric calibration of the VVDS sample is better than ~10% rms in optimal weather conditions, we favour the use of the EW[OII] instead of line fluxes to estimate the SFR. In this way we minimise the dependency of our estimates on less optimal weather conditions and slit losses (see for details Le Fèvre et al. 2005).

There are three main caveats for the reliability of the SFR conversion obtained from EW[OII] using Eq. (1) over the whole redshift interval ($0.5 \leq z \leq 1.3$): the uncertainty on the fraction of active galactic nuclei (AGN) present in our sample, the cosmic evolution of metallicity, and the amount of extinction.

One risk in interpreting line measurements as proxy for star-formation activity is the contamination arising from the presence of an AGN in the central region of a galaxy. In this case, the emission lines in the spectrum would be a mixture of contributions from both the AGN and star formation. We removed from our final sample the spectroscopically confirmed broad-line AGNs. We estimate a contamination from type II AGN-dominated galaxies on the order of 7% over the redshift range explored. This fraction has been estimated using the standard line ratio diagnostic tools, i.e. [OIII]λ5007/Hβ vs. [OII]λ3727/Hβ in the redshift interval $0.5 < z < 0.8$ and new diagnostics using [OII]λ3727, [NeIII]λ3869 and Hδ in the redshift interval $0.9 < z < 1.3$ (for details we refer to Lamareille et al. in prep. and Perez-Montero et al., in prep.). However, given the very significant uncertainty that is affecting the identification of these narrow-line AGNs and their relatively small number, we have decided not to remove them from the sample.

Another possible limitation we face in converting EW[OII] into star formation estimates is related to the metallicity and its cosmic evolution, that could result into a systematic change of line intensities with redshift even if the star formation activity were to remain constant. Mouhcine et al. (2005) have shown that a variation of the metallicity by a factor of 4 can produce a variation of a factor of about 3 in the reddening-corrected [OII]λ3727/Hα flux ratio (see Fig. 12 in Mouhcine et al. 2005). This relation however has an opposite behaviour for different metal regimes. We have the scenario in which the [OII]λ3727/Hα flux ratio increases with metallicity in metal-poor galaxies which are typically low-mass objects ($\log(M/M_\odot) < 10$, ~0.2 $Z_\odot$), and it decreases with metallicity in metal-rich galaxies which are typically massive galaxies ($\log(M/M_\odot) > 11$, 1.4 $Z_\odot$), see e.g. Gallazzi et al. (2005). As for the direct effect of metallicity evolution on line strength, there is still considerable debate about the details of the evolution of the mass-metallicity relation. Savaglio et al. (2005) find very little change in metallicity for massive, already high-metallicity systems, up to $z \sim 1$. They find a significant overall increase of metallicity for low-mass, generally low-metallicity objects. On the contrary, Lamareille et al. (2006) observe a general decrease of metallicity which is essentially independent from galaxy mass, while the VVDS data (Lamareille et al. in prep.) show some indication of a smaller change of metallicity for low-mass systems than for high-mass ones. Overall these studies are concordant in finding an evolution of the metallicity within a factor of 2 up to $z \sim 1$. This would imply an uncertainty of less than a factor of two in our star formation rate estimates. As the observed variations in star formation activity are significantly larger than this uncertainty, and the metallicity estimates we can obtain are also highly uncertain because of the low spectral resolution and low S/N of our spectra, we prefer not to correct our [OII] measurements for metallicity variations.

Finally, we also have to consider the effects of dust extinction on our SFR estimates, although they are reduced by the use of equivalent widths instead of line fluxes. The observed line and continuum fluxes involved in the determination of the equivalent width are both affected by the diffuse dust extinction

within the galaxy, and the only differential effect would be due to localised extinction within HII regions, that should account for only a minor fraction of the total dust extinction within a galaxy (Kennicutt 1989; Charlot & Longhetti 2001). To account for the dust attenuation we corrected the EW[OII] by the amount of the extinction provided by our template fitting using PEGASE (Fioc & Rocca-Volmerange 1997, see next section). The correction values obtained with this method vary within the interval EW[OII]$_{corr}$/EW[OII] $\in$ [1−2.7].

To the caveats we already mentioned, for sake of completeness we should also add the possible uncertainties derived from the unknown physical condition of the ionizing gas and those related to the difference between our sample and the one originally used to calibrate Hα/[OII] in Eq. (1) (Guzman et al. 1997).

3.4. Stellar mass estimates

We obtain the stellar masses for our galaxy sample by fitting the photometric and spectroscopic data with a grid of stellar population synthesis models generated by the PEGASE2 population synthesis code (Fioc & Rocca-Volmerange 1999, [astro-ph/9912179]; Fioc & Rocca-Volmerange 1997), and using the GOSSIP Spectral Energy Distribution tool (Franzetti 2005). The models were produced assuming a Salpeter initial mass function (Salpeter 1955) to allow an easy comparison with previous analyses (e.g. Brinchmann & Ellis 2000; Fontana et al. 2004). The use of other prescriptions for initial mass functions (IMFs) does not introduce any significant difference in the redshift evolution of the mass estimate in the z interval explored as the ratio between masses derived with e.g. a Salpeter IMF and the ones derived with a Chabrier IMF is close to a constant for most star formation histories (see Pozzetti et al. 2007, hereafter P07). We use a set of delayed exponential star formation histories (see Eq. (3) in Gavazzi et al. 2002) with galaxy ages, t, in the range from 0.1 to 15 Gyr, and star formation time-scales, τ, between 0.1 and 25 Gyr. Internal dust extinction is handled self-consistently with the star formation activity by the PEGASE2 code and no burst component has been added.

Stellar masses obtained with this method were compared with other estimates based on the fitting of the photometric data only and photometric plus spectroscopic data with Bruzual & Charlot (2003) models derived using different families of star formation histories. We find the various estimates to be consistent with each other in the redshift interval investigated. We estimate a statistical uncertainty on the mass estimate of approximately 0.2 dex. In particular, our methodology is equivalent to the smooth SFHs method described in P07 even if they adopt an exponentially decreasing star formation history and Bruzual & Charlot (2003) models, rather than a delayed exponential star formation history and PEGASE2 population synthesis models as in this work. The photometry coverage was improved with respect to P07, and it now includes UKIDSS NIR (JK bands) photometry (Lawrence et al. 2007) and SPITZER-IRAC (3.6, 4.5, 5.8, and 8 μm) photometry from the SWIRE survey (Lonsdale et al. 2003). Even if our stellar masses are well consistent with the ones by P07, the new photometry improves the mass determination avoiding the need for any further statistical correction, as made in P07 because of the lack of NIR photometry in about half of the sample.

Stellar mass completeness limits have been estimated using the same stellar population synthesis models described above to predict apparent I-band magnitudes for galaxies with different star formation histories (and therefore different mass to light ratios) as a function of redshift. Comparing these predicted magnitudes with the magnitude limit used to select the survey spectroscopic sample we estimate that we can observe galaxies above $\log(M_\star) \simeq 9.6, 9.9, 10.5\ M_\odot$ for $z \in$ [0.5−0.7], [0.7−1], [1−1.3], respectively. These stellar mass limits correspond to a completeness >80% for the early-type population and more than 95% for late-type galaxies.

We refer to P07 for the method adopted to construct the stellar mass function. Here we briefly describe the most important points. We derive the mass functions using the classical non-parametric $1/V_{max}$ formalism following Schmidt (1968) and Felten (1976). We use for the fit the Schechter function limiting ourselves above the 80% completeness stellar mass limits for the two different population examined. In the estimate of the mass function we take into account also the incompleteness resulting from non-targeted sources in our spectroscopic observations and from spectroscopic failures.

4. Results

4.1. Evolution of stellar ages with stellar mass

In the local Universe there is a well established observational evidence that while young galaxies are preferentially low-mass systems, old galaxies are mostly massive systems. In particular, Kauffmann et al. (2003b) identify in their Fig. 2 the population of the first peak of the D_n4000 distribution observed at $D_n4000 \sim 1.3$ as emission line objects with a mean stellar age of 1−3 Gyr and low stellar mass ($\log(M/M_\odot) < 10.4$). The second peak at $D_n4000 \sim 1.85$ corresponds instead to old (>10 Gyr), massive ellipticals.

Figure 1 shows the histogram of the D_n4000 distribution in different intervals of stellar masses and redshifts as indicated on the top and on the right, respectively. For the VVDS-F02 data (rows 2−4) the histograms are corrected for non-targeted sources in our spectroscopic observations and for spectroscopic failures (the corrected total number and the actual number of observed galaxies are reported in the first and second lines, respectively, at the top of each panel).

To allow a direct comparison with the local Universe, the first row of Fig. 1 shows the D_n4000 distribution as derived from a local sample of SDSS DR4 galaxies (Adelman-McCarthy et al. 2006) within the same interval of stellar masses as ours (properly rescaled to account for the different IMFs). This plot enables us to explore the presence of any relation between stellar ages and stellar masses in the distant Universe. The vertical dotted lines represent the cutoff at $D_n4000 = 1.5$ adopted to sub-divide our objects in early- and late-types, as described in the Sect. 3.2. The vertical dashed line in each panel is the median of the D_n4000 distribution in that particular stellar mass interval and redshift bin (see Table 1). In the low-mass interval at high redshift the incompleteness for early-type galaxies affects the high value tail of the D_n4000 distribution, while it does not strongly affect the median values, dominated by late-type galaxies.

The first evidence shown by Fig. 1 is the different behaviour of the D_n4000 distribution for the five bins of stellar mass explored. They show a clear dependency of the stellar age as inferred by D_n4000 values on the stellar mass that holds at all epochs up to $z \sim 1.3$. Even at the highest redshift bin investigated the D_n4000 distributions closely follow the behaviour observed in the local Universe. Low-mass galaxies have small D_n4000 values and, as mass increases, the galaxy distribution moves to larger D_n4000 values. At any fixed redshift bin, the relative abundance of early-type galaxies ($D_n4000 > 1.5$) increases as mass increases. The largest D_n4000 values, and thus the oldest
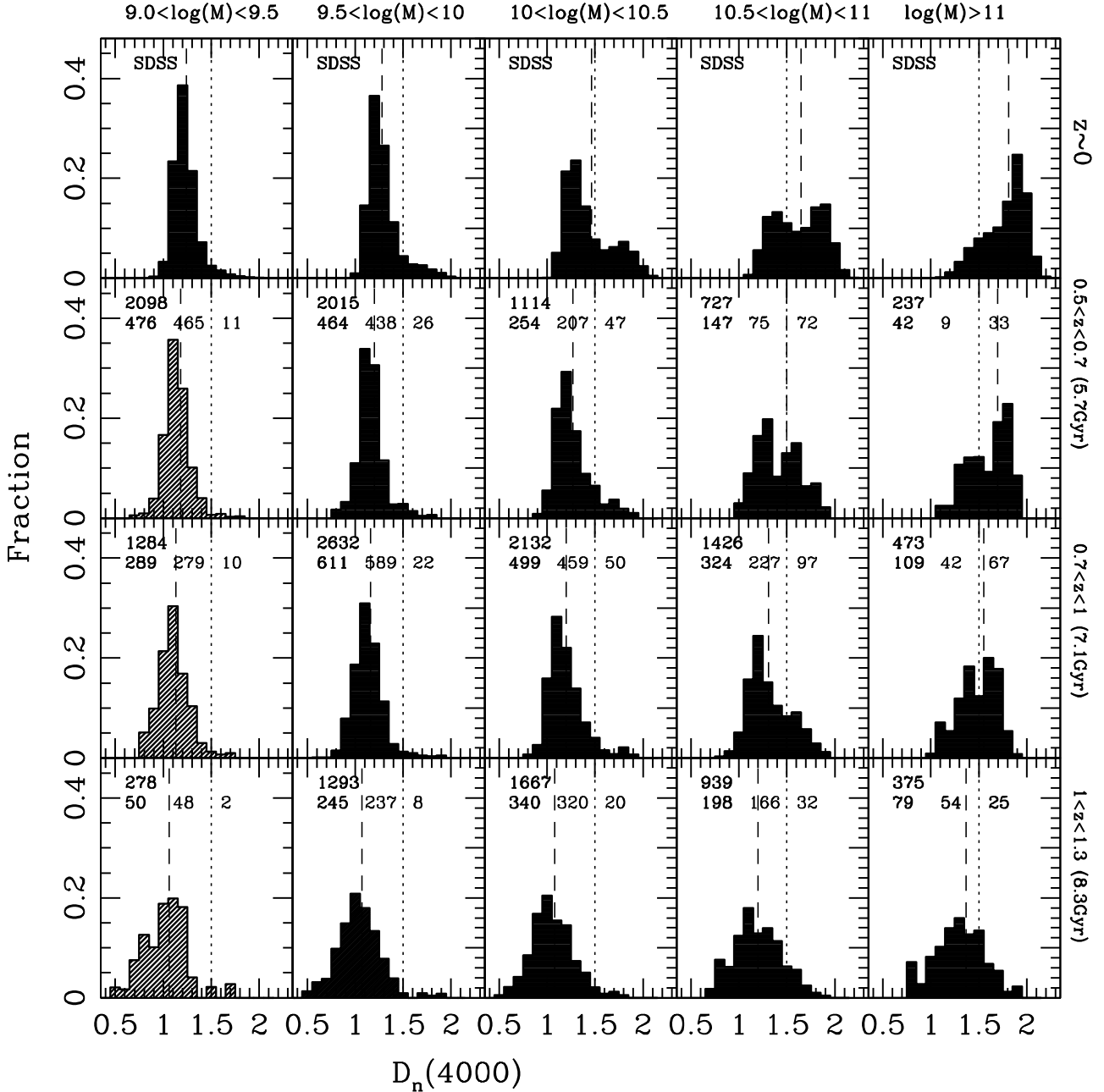
Fig. 1. Histograms showing the fraction of VVDS-F02 galaxies as a function of D_n4000 in five different ranges of stellar mass and in three redshift bins (0.5–0.7, 0.7–1.0, 1.0–1.3, rows 2–4). We plot as a comparison in the first row the D_n4000 galaxy distribution for the local Universe ($z \sim 0$) from the SDSS DR4 (Adelman-McCarthy et al. 2006). The counts corrected for non-targeted sources in our spectroscopic observations and for spectroscopic failures (unidentified sources) following Ilbert et al. (2005) are reported in the first line at the top of each panel, the observed counts of (total, late-, and early-type) galaxies in the second line. The vertical dotted lines at $D_n4000 = 1.5$ represent the adopted separation between early- and late-type galaxies. The vertical dashed lines represent the median D_n4000 distribution in each panel. The panels in the first column dominated mostly entirely by late-type galaxies have dashed D_n4000 distribution when the mass completeness for the late-type population is less than 50%.

underlying stellar populations or early-type galaxies following Sect. 3.2, are hosted in the most massive galaxies at all redshifts up to $z \sim 1.3$.

Another striking evidence coming from Fig. 1 is that for the lower mass galaxies ($\log(M/M_\odot) < 10$) the shape of the D_n4000 distribution does not seem to evolve with time between $z \sim 1$ and $z \sim 0$. For these galaxies the D_n4000 distribution is peaked around $D_n4000 \sim 1.1$ in all redshift bins, suggesting a good correspondence up to high redshifts between a low stellar mass and a young underlying stellar population. Intermediate and

high-mass galaxies show significant evolution with redshift at $z > 0.7$ as testified by the progressive shift of the median value (dashed line in Fig. 1). As cosmic time goes by, for stellar mass larger than $\log(M/M_\odot) > 10$ galaxies populate progressively the locus of larger D_n4000 values and a secondary peak emerges in the D_n4000 distribution. The gradual accumulation of the secondary peak is a process started at early epochs that continues efficiently down to the local Universe.

We find an age-stellar mass relation with low-mass galaxies having younger stellar populations and more massive galaxies
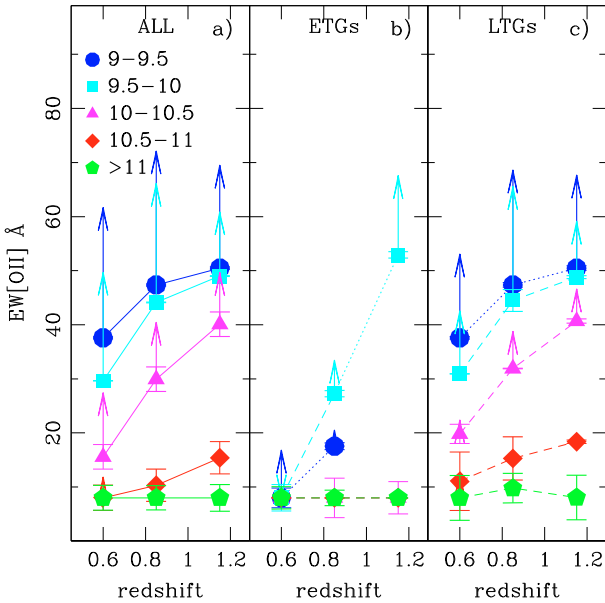
Fig. 2. The median *EW*[OII] as a function of the redshift for our VVDS-F02 sample **a)** in bins of stellar masses, coded as follows: $9.0 < \log(M/M_\odot) \leq 9.5$ (blue, circle), $9.5 < \log(M/M_\odot) \leq 10$ (cyan, square), $10 < \log(M/M_\odot) \leq 10.5$ (magenta, triangle), $10.5 < \log(M/M_\odot) \leq 11$ (red, diamond), and $\log(M/M_\odot) > 11$ (green, pentagon). The same visualization is presented for the spectroscopic early- **b)** and late-type galaxies **c)**. The symbols represent the observed *EW*[OII] and the arrows the dust corrected *EW*[OII]. The points are connected with dashed (dotted) lines when the mass completeness of each population is above (below) 50%.

Table 1. D_n4000 median distribution.

z	$10^{9-9.5}\,M_\odot$	$10^{9.5-10}\,M_\odot$	$10^{10-10.5}\,M_\odot$	$10^{10.5-11}\,M_\odot$	$10^{>11}\,M_\odot$
~0	1.24 ± 0.00	1.28 ± 0.00	1.46 ± 0.00	1.66 ± 0.00	1.81 ± 0.00
$0.5-0.7$	1.18 ± 0.01	1.20 ± 0.01	1.27 ± 0.01	1.50 ± 0.02	1.69 ± 0.02
$0.7-1.0$	1.13 ± 0.01	1.16 ± 0.01	1.21 ± 0.01	1.31 ± 0.01	1.55 ± 0.02
$1.0-1.3$	1.07 ± 0.04	1.07 ± 0.02	1.09 ± 0.01	1.20 ± 0.02	1.37 ± 0.02

Notes: D_n4000 median values in five intervals of stellar mass and three redshift bins for our VVDS-F02 sample. The error quoted in each interval represents the error on the median distribution using a statistical Jackknife technique. The median values of the D_n4000 distribution in a nearby galaxy sample (SDSS DR4) are also listed.

possessing older stellar population. This correlation, originally observed in the local Universe by e.g. Kauffmann et al. (2003b), seems to hold up to $z = 1.3$. Our findings on the progressive accumulation with time of massive galaxies with large D_n4000 values can be interpreted in the framework of a top-down picture of the stellar mass assembly history of galaxies, also termed *assembly downsizing*. With this terminology we refer to the galactic property that regardless of type, massive galaxies are fully assembled at earlier times, with less massive galaxies assembled later (when mass is defined as stellar mass). Note that here we make no statement about how the stellar mass was aggregated, as both merging and star formation can contribute to the assembly process. However we will argue in Sect. 4.5 that galaxy major merger does not seem to be a fundamental mechanism, at least at $z < 1$.

Evidence of this top-down stellar mass assembly is already present in literature, e.g. Thomas et al. (2005); Cimatti et al. (2006); Bundy et al. (2006). Studies on stellar age, metallicity,

and cosmic star formation at $z \sim 0$ prove that stars in massive galaxies were formed long ago and over a short period of time (e.g. Thomas et al. 2005; Heavens et al. 2004; Jimenez et al. 2005). At high redshifts the reddest galaxies already possess old ages (>1 Gyr), establishing their formation epoch at $z > 2$ (McCarthy et al. 2004; Cimatti et al. 2004). Furthermore, massive proto-disk galaxies already exist at $z \sim 2-3$ (e.g. Labbé et al. 2003; Stockton et al. 2004; Förster Schreiber et al. 2006; Genzel et al. 2006). On the contrary, the underlying stellar ages of late-type galaxies apparently do not show evolution. This observation is probably justified by a continuous and efficient formation rate of new stars (see next Sect. 4.3) as discussed also in other studies (Arnouts et al. 2007; Faber et al. 2007).

Theoretical models, however, predict that stars in an object can be born in a different place from where they finally end up (e.g. de Lucia et al. 2006). Even if we observe a downsizing signal, stars born long ago in several objects could still coalesce into a single object in a hierarchical way making the concepts of assembly of a system and assembly of its stars different. However, to be able to test this theoretical prediction we need to wait for the next generation of surveys and more detailed semi-analytical models.

Based on our phenomenological approach we can conclude as follows. Our sample shows to which extent the stellar mass drives the galaxy evolution. For the first time we present a direct comparison of stellar ages and stellar masses of galaxies over the last 8 Gyr extending to higher redshift the seminal work by Kauffmann et al. (2003b) on $z = 0$ galaxies.

4.2. SFR dependence on stellar mass and redshift

A cosmic decline of the star formation activity has been presented in several studies, starting from field redshift surveys by Lilly et al. (1996); Madau et al. (1996). Nowadays, the knowledge of the cosmic star formation history out to redshift $z \sim 1$ is quite profound (Hopkins & Beacom 2006, and references therein). However many aspects of galaxy evolution, like the contribution to galaxy mass assembly of various categories of galaxies, still need to be understood (see for details e.g. Cimatti et al. 2006).

Panel a of Fig. 2 shows the median distribution of *EW*[OII] in the redshift interval $z = 0.5-1.3$ as a function of the stellar mass. Galaxies with no *EW*[OII] detection are taken into account in the median computation assigning to them the *EW*[OII] upper limit estimated from the 1σ measurement uncertainty. Interpreting the *EW*[OII] as a proxy for star formation activity, we can infer that the latter has a clear redshift evolution which is strongly modulated by stellar mass. We observe the already well established global star formation decline from $z \sim 1$ to the present epoch, and also that within a given redshift bin the smaller the stellar mass of the galaxy, the more actively it is forming stars.

These results are in excellent agreement with the findings by Feulner et al. (2005a) based on a large sample of 9000 galaxies although with only photometric redshifts from the FORS Deep Field and the GOODS-S field. They show a similar trend for the SSFRs at different stellar mass intervals with no contribution to the stellar mass growth for massive galaxies (cf. Fig. 2 in Feulner et al. 2005a). We also find an excellent agreement in the common redshift range with the study of 207 galaxies from the spectroscopic GDDS (Juneau et al. 2005). They show that massive GDDS galaxies ($\log(M/M_\odot) > 10.2$) are in a quiescent mode, and lower mass GGDS galaxies in a burst phase. Similar results have been obtained by Zheng et al. (2007) using $\sim$15 000 COMBO-17 galaxies with photometric redshifts, supplemented

by ultraviolet and infrared data to account for otherwise undetected star formation activity.

Our results, being obtained on a large spectroscopic sample, put on firmer grounds the results previously found using photometric galaxy catalogues or smaller spectroscopic surveys: the star formation in massive systems is at very low values since $z \sim 1-1.3$, while star formation increases when considering less massive systems at each redshift bin explored.

Panels b and c of Fig. 2 show what happens when one considers early- and late-type galaxies separately. Very massive galaxies ($\log(M/M_\odot) > 11$) irrespective of their spectral type show negligible star formation activity at each redshift bin probed. Moving to lower masses, galaxies of different spectral classification show different behaviour (both in slope and normalization of EW[OII] values). This result holds over the entire inspected redshift range. In panel b at masses lower than $\log(M/M_\odot) \sim 10$ there is an indication of the presence of galaxies with an old underlying stellar population (ETGs) and non-negligible levels of [OII]. However, given a number of considerations, including the larger mass incompleteness and the small number statistics for this class of objects (see numbers quoted in Fig. 1), one should be cautious in putting too much weight on this result. Interestingly, with our classification scheme we find a lower contamination of star forming galaxies among early-type objects than reported in previous studies (5% vs. 20−50%, see Strateva et al. 2001; Franzetti et al. 2007; Cimatti et al. 2002; Kriek et al. 2006). This could be the result of our classification criterion that, being based on D_n4000, allows rejecting e.g. dusty-star forming EROs that possess red colours but low D_n4000 values (Mignoli et al. 2005). Another concern we need to stress is the possible contamination from the type II AGN-dominated galaxies as they might still be present in our sample. A number of studies have recently shown that emission lines in early-type galaxies at $z = 0$ are mainly due to AGN rather than to star formation activity (e.g. Weiner et al. 2007). Therefore we can not exclude the possibility that even the 5% of early-type galaxies with non-negligible star formation could actually be AGNs, thus casting doubt on the possibility of interpreting EW[OII] as star formation indicator for low-mass early-type galaxies in panel b of Fig. 2.

Panel c of Fig. 2 shows clear trends for late-type galaxies both as a function of redshift and of mass. Galaxies have a stronger EW[OII] going back in cosmic time and this trend is steeper for less massive galaxies. The trends visible in panel a of Fig. 2 are therefore driven by the late-type galaxies.

An important piece of information about the global star formation history of galaxies becomes apparent when comparing the results summarised in Figs. 1 and 2. It is known that the D_n4000 strength is the result of the cumulative star formation history of a galaxy. As already discussed in Sect. 3.2, D_n4000 values below 1.5 are indicative of significant star formation activity within the last 1 Gyr, while values above 1.5 are associated to galaxies that have finished forming their stars at least 1 Gyr ago, and are therefore evolving mostly, if not exclusively, via the passive evolution of their stellar population. Instead the [OII] line is sampling only the instantaneous star formation activity, because the ionizing flux in HII regions is provided almost entirely by massive stars ($\log(M/M_\odot) > 10$) with lifetimes limited to 20 Myr or less. Therefore, the star formation time-scales probed with the D_n4000 and the [OII] equivalent width are very different. Despite their difference, however, there is a general agreement between them: both indicators consistently point towards a star formation history peaked in the past for massive galaxies, with little or no residual star formation taking place at the epoch of the observation. Vice-versa most of the low-mass

systems show just the opposite characteristics: almost all galaxies in this subset have small D_n4000 and a rather strong current star formation activity.

In our sample massive galaxies are the only subset of the galaxy population that shows a significant presence of objects with large D_n4000, and all these objects have also very low or null recent star formation activity. For low-mass galaxies both indicators suggest a general picture of extended star formation activity. These galaxies are dominated by the young stellar population at all epochs (although with this kind of analysis we cannot say anything about their epoch of formation, of course).

The very good agreement observed for massive objects between the instantaneous and the integrated star formation indicators can be understood by assuming that the dominant mode of star formation activity for these systems after an initial burst is a continuous one, with relatively smooth variations in time, and with no significant contribution from a secondary strong burst. A similar conclusion has been presented recently by Noeske et al. (2007), based on their analysis of the AEGIS survey data.

We notice that a somewhat similar dependence of burst activity on galaxy stellar mass has been observed in the SDSS data by Kauffmann et al. (2003a), although their most recent work (Kauffmann et al. 2006) indicates a more important role for galaxy surface mass density than for total mass in regulating star formation activity.

The agreement between the two star formation indicators would be violated by the small fraction of low-mass spectral early-type galaxies where a large D_n4000 value, that points towards a predominantly old stellar population, is coupled with a significant [OII] emission, should this feature be indicative of ongoing star formation activity (see Fig. 2, panel b). We have already listed a series of caveats on the risks of over-interpreting the significance of such population. It is nevertheless worth mentioning that it is possible to reproduce such a dichotomy between the two indicators when the starburst is involving only a very small fraction of the galaxy total stellar population (approximately less than 2% by mass, but the exact value for this limit depends on the amount of dimming introduced by dust extinction localised in the star-forming regions).

The general picture which emerges from the Figs. 1 and 2 follows the classical concept of downsizing as firstly suggested by Cowie et al. (1996). In this framework one expects a continuous growth in stellar mass of low-mass galaxies with time while the massive galaxies have stopped to form stars at early epochs. This galaxy attitude is also termed downsizing in star formation, or in time (Neistein et al. 2006). Most of the claims of downsizing in the literature fall in this category (e.g. Bauer et al. 2005; Juneau et al. 2005; Feulner et al. 2005a,b; Tresse et al. 2006).

4.3. Stellar mass assembly in early- and late-type galaxies

We show in Fig. 3 the stellar mass function (MF) in three redshift bins both for early- and late-type galaxies according to the spectral classification introduced in Sect. 3.2. We also show the total mass function for each redshift bin, but we refer to P07 for a detailed discussion on the VVDS-F02 mass function. The parameters of the Schechter fit (α, $M^*_{\rm star}$, ϕ^*) for early- and late-type galaxy samples are listed in Table 2 along with their uncertainties. As the interval $0.7 \le z \le 1$ provides the best sampling of the overall galaxy population we adopt the characteristic mass ($M^*_{\rm star}$) of late-type galaxies measured in this bin for the lower redshift one (where we do not sample well enough the high-mass end of the population), and the slopes of both early- and late-type MFs measured in this bin for the higher redshift one.

Table 2. Schechter fit parameters.

z range		α	$\log M_{star}^*$ $(h_{70}\ M_\odot)$	ϕ^* $(10^{-3} h_{70}^3\ \mathrm{Mpc}^{-3})$		α	$\log M_{star}^*$ $(h_{70}\ M_\odot)$	ϕ^* $(10^{-3} h_{70}^3\ \mathrm{Mpc}^{-3})$	$\log M_{tr}$
$0.5 < z < 0.7$	ETG	$-0.36^{+0.19}_{-0.19}$	$11.06^{+0.12}_{-0.10}$	$1.50^{+0.25}_{-0.30}$	LTG	$-1.44^{+0.11}_{-0.09}$	10.96	$1.05^{+0.5}_{-0.35}$	10.87
$0.7 < z < 1.0$		$-0.46^{+0.20}_{-0.19}$	$11.09^{+0.12}_{-0.10}$	$0.80^{+0.15}_{-0.15}$		$-1.34^{+0.14}_{-0.12}$	$10.96^{+0.15}_{-0.13}$	$1.30^{+0.6}_{-0.45}$	11.11
$1.0 < z < 1.3$		-0.46	$11.20^{+0.07}_{-0.06}$	$0.25^{+0.15}_{-0.15}$		-1.34	$11.08^{+0.07}_{-0.08}$	$0.75^{+0.1}_{-0.10}$	11.42

Notes: The listed values are computed on the early-type (ETG) and late-type (LTG) samples using a classification scheme based on the age-estimator D_n4000 (see Sect. 3.2).
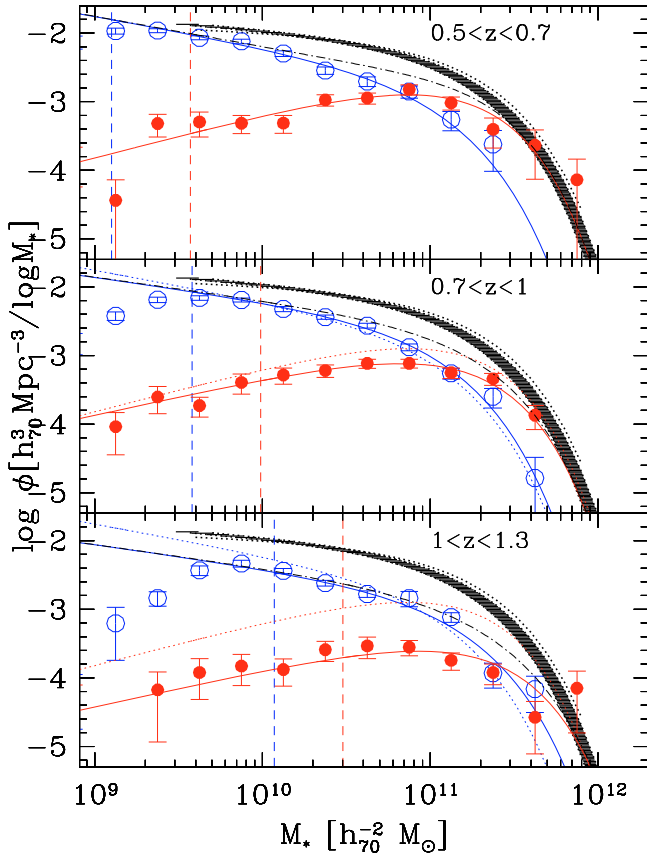

Fig. 3. Stellar mass function for the spectroscopically classified late-type (empty circles) and early-type (filled circles) galaxies from VVDS-F02 sample. The total mass function for each redshift bin is plotted as dashed-point line, while in each panel we also report the total local MF range, using Cole et al. (2001) and Bell et al. (2003) (shaded region and dotted line, respectively). The stellar mass functions of the two spectral types of the lowest redshift bin are over-plotted at each panel as dotted lines. The vertical dashed lines represent the 80% completeness limits for the two spectral types.

The vertical dashed line in each panel represents our mass limit in that redshift bin (see Sect. 3.4). To judge the evolution in the three redshift intervals we over-plot the Schechter fits to early- and late-type stellar mass functions of the lowest redshift bin at each panel (red and blue, dotted lines), and the total local MF range, using Cole et al. (2001) and Bell et al. (2003) (shaded region and dotted line, respectively).

Comparing the total galaxy MF of Fig. 3 to the local MF, we find a strong evolution depending on galaxy stellar mass confirming previous results of P07. Galaxies with stellar masses larger than $\log (M/M_\odot) > 11$ show an evolution on the order of 30−50% up to $z \sim 0.7$−1.0 and a faster evolution above $z \sim 1$,

while the number density of less massive galaxies decreases more continuously with redshift.

Our main focus is on the contribution of the different galaxy populations to the total mass function and to its evolution. For stellar masses larger than $\log (M/M_\odot) > 11.4$ most of the galaxies have an early-type classification over all the redshift range explored ($0.5 \leq z \leq 1.3$) and no massive late-type galaxies ($\log (M/M_\odot) > 11.5$) are observed at $z < 0.7$ within our sample. Figure 3 also shows that at the intermediate/low-mass tail ($\log (M/M_\odot) < 10$) the number density of both early- and late-type galaxies increases with cosmic time: by a factor of ~ 1.6 at $\log (M) = 10\ M_\odot$ within the redshift range explored (and a factor of 3 compared to local MFs) for late-type galaxies, and more strongly for early-type ones (by a factor of 5 within the redshift range explored). We can therefore conclude that while the massive end of the mass function is mainly dominated by early-type galaxies up to $z \sim 1$, late-type galaxies mostly contribute to the intermediate/low-mass part ($<10.5\ M_\odot$) of the mass function at all redshifts. Furthermore the abundance of massive early-type galaxies ($>11\ M_\odot$) increases with cosmic time but with a declining rate at lower redshift. There is also an indication of a small decreasing of the massive tail of the late-type mass function from $z = 1.3$ to $z = 0.5$.

According to our results, the stellar mass function shows an increasing (decreasing) relative contribution of massive early (late) type galaxies, and a general increase, but at different rates and depending on the mass, of both early and late-type galaxies with cosmic time. These results imply a redistribution of the stellar mass amongst the spectral types with a declining contribution to the overall mass function of massive late-type with time associated with an increasing number density of intermediate-massive early-type galaxies.

The overall picture emerging from our stellar mass function agrees quite well with previous results (e.g. Fontana et al. 2004; Bundy et al. 2006). Generally the stellar mass function of late-type galaxies agrees very well in all studies. As far as the stellar mass function for the early-type galaxies is concerned the better agreement is obtained with the study by Fontana et al. (2004) who use a spectral classification, instead of a rest-frame colour scheme (Bundy et al. 2006). A slightly worse concordance is found for the early-type galaxy densities at $z > 0.7$ with Bundy et al. which are larger than the one computed in our study. Furthermore, we find a stronger evolution of early-type massive galaxies at $z > 1$ compared to the one measured for red galaxies in Bundy et al.

The mass redistribution of morphological types as a function of redshift was first noticed by Brinchmann & Ellis (2000) computing the stellar mass density in a small sample of I-selected galaxies with spectroscopic redshifts and infrared photometry. Using Hubble Space Telescope morphologies, Brinchmann & Ellis (2000) observed a decline in the mass density of irregular galaxies from $z \simeq 1$ to today either associated to a transformation

into regular morphologies and/or to merging mechanisms. These results were confirmed by Bundy et al. (2005) using a sample of approximately two thousand morphologically-classified galaxies from GOODS (Giavalisco et al. 2004). Later on Bundy et al. (2006) provided further support to the stellar mass redistribution using the DEEP2 spectroscopic sample producing type-dependent stellar mass functions based on rest-frame colours. Further evidence can also be found in other studies. For example, a similar modest change in abundance of massive early-type up to $z \sim 1$ was found in the K20 sample which has a high redshift accuracy and a spectral classification similar to ours (Fontana et al. 2004). The constancy in blue populations and the increasing trend of the red sequence classified according to $(NUV - r)$ colours have been observed in a study of stellar mass density by Arnouts et al. (2007), and previously observed by Borch et al. (2006) and Martin et al. (2007).

We observe in Fig. 3 a downward transition with time of the threshold in the stellar mass above which the early-type galaxies become dominant in the relative contribution to the total stellar mass function. This characteristic mass, or transition mass (M_{tr} reported in Table 2), was detected in the local Universe around $3 \times 10^{10} \, M_\odot$ (Kauffmann et al. 2003b; Baldry et al. 2004). Bundy et al. (2006) report its evolution with cosmic time using three different methods to define the two galaxy categories: galaxies are partitioned according to rest-frame colours, to the star formation rate and to morphological properties. Our findings based on the D_n4000 index are in between those obtained dividing the galaxies by colours and by morphology in Bundy et al. (2006) and show a similar trend in cosmic time. A less steep evolution is observed when considering the classification obtained by Bundy et al. (2006) with the SFR indicator.

To better show the differential evolution of galaxies and the general redistribution in stellar mass among galaxies we plot in Fig. 4 the evolution of the early-type galaxy fraction over the entire (early- and late-type) population for different stellar mass bins as a function of redshift. Both observed counts and Schechter fitted values are used in the computation and plotted with different symbols. The error-bars include both the uncertainties in the spectral measurements and the effect of changing the classification due to the D_n4000 errors. As in Fig. 1 we report the reference points at $z \sim 0$ from a local galaxy sample (SDSS DR4).

Figure 4 clearly shows how the evolution of the relative abundances of early- and late-type galaxies strongly depends on galaxy stellar mass. The relative fraction of the most massive galaxies ($\log(M) > 11 \, M_\odot$) significantly changes with cosmic time, between $z = 1.2$ and $z = 0.85$ due to both the decrease of massive late-type and the increase of massive early-type galaxies, followed by a flattening below $z = 0.85$, when this second population becomes dominant in this mass regime. A similar flattening is present at $z < 0.6$ for galaxies with $\log(M) > 10.5-11 \, M_\odot$. A more continuous evolutionary trend is suggested for the relative fraction within the less massive population ($<10.5 \, M_\odot$): both late- and early-type densities increase but the first category of galaxies is always dominant at this stellar mass regime (Fig. 3).

As these measured ratios could be affected both by different mass completeness limits for early and late-type galaxies (as the VVDS is a magnitude limited survey) and by any incompleteness in the global spectroscopic sample, we derive the relative fraction of early-type galaxies also integrating the best fit Schechter function. The agreement between the observed ratios and the ones derived by the Schechter integration shows that our results are robust.
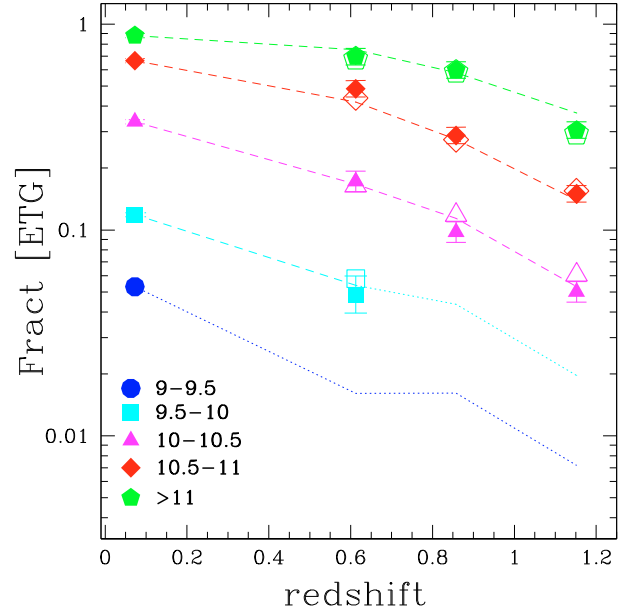

Fig. 4. The evolution of the fraction of galaxies classified spectroscopically as early-type in different mass intervals. The mass bins are coded as follows: $9.0 < \log(M/M_\odot) \leq 9.5$ (blue, circle), $9.5 < \log(M/M_\odot) \leq 10$ (cyan, square), $10 < \log(M/M_\odot) \leq 10.5$ (magenta, triangle), $10.5 < \log(M/M_\odot) < 11$ (red, diamond), $\log(M/M_\odot) > 11$ (green, pentagon). Filled symbols represent the counts of observed galaxies, while the open symbols represent the counts derived from $1/V_{max}$ formalism. The dashed lines are the Schechter fitted values to the stellar mass function (dotted in the case of mass completeness for early-type galaxies below 50%.) The points at $z \sim 0$ are our SDSS reference points.

To summarise, our results suggest a galaxy mass assembly history with a mild evolution with redshift in number density (P07) for very massive galaxies ($>11.4 \, M_\odot$), which are mainly constituted by early-type galaxies up to the redshift sampled ($z < 1.3$). Since the relative fraction of massive early- and late-type galaxies evolves with cosmic time we witness a spectral transformation of late-type systems into old massive galaxies at lower redshift. In Sect. 4.5 we analyse the efficiency of this mass assembly process driven by the star formation rate observed in galaxies.

4.4. Influence of cosmic variance

An intrinsic source of uncertainty in any estimate of number densities from a finite-size survey is represented by the variance induced by density fluctuations on scales comparable to, or larger than, that of the sampled volume. This is what is commonly termed "cosmic variance". It inversely depends on the sample volume and directly on the two-point correlation function of the class of galaxies under analysis. This cosmic variance will introduce a systematic effect on the overall amplitude of our mass function. The significance of this effect needs to be evaluated. This can be obtained in our case with fairly good accuracy for the three redshift bins of VVDS-F02 used here, since we already know the clustering properties of both the early- and late-type galaxy population over the whole range covered by the survey (Meneux et al. 2006).

Following Peebles (1980) and Somerville et al. (2004), under the assumption of a power-law correlation function

Table 3. Relative rms error on galaxy number densities expected from cosmic variance in the three redshift samples.

Type	σ_{counts}		
	$0.5 < z < 0.7$	$0.7 < z < 1$	$1 < z < 1.3$
Early	0.20	0.15	0.14
Late	0.17	0.14	0.13

$\xi(r) = (r/r_0)^{-\gamma}$ the *relative* variance of galaxy counts over a given volume with radius R can be expressed as

$$\sigma_R^2 = J_2 \, (R/r_0)^{-\gamma}. \tag{2}$$

Here J_2 is a classical integral over the two-point correlation function as defined in Peebles (1980), which in the power-law approximation can be expressed as

$$J_2 = 72/[(3 - \gamma)(4 - \gamma)(6 - \gamma)2^\gamma]. \tag{3}$$

In the case of a non-spherical volume V, we can nevertheless define an equivalent radius as $R = (3V/4\pi)^{1/3}$. For our three samples, this corresponds to $R = 34$, 45 and 49 h^{-1} Mpc, respectively. From Meneux et al. (2006), we know that, to sufficient approximation, the correlation length r_0 and slope γ of $\xi(r)$ do not evolve significantly, being $r_0 \simeq 4(2.5) \, h^{-1}$ Mpc and $\gamma = 1.8$ (1.5) for early- (late-)type galaxies respectively, over the full redshift range under investigation. Thus, we have all the ingredients to use Eqs. (2) and (3) to estimate the expected rms relative error on the measured densities, $\sigma_{counts} = \sqrt{\sigma_R^2}$, for each of the three samples. The results are reported in Table 3. The listed values indicate that the systematic error on our estimates of the mass due to cosmic variance is expected to be between 13 and 20%. This is fully consistent with the result we have obtained by splitting the sample into two parts and recomputing the mass functions separately for the two subsamples. The agreement between these two independent estimates allows us to conclude that our conclusions are robust with respect to cosmic variance.

4.5. Efficiency in the stellar mass assembly process

In the case of dry merging – merging of quiescent galaxies without gas (star formation) involved – the age of the galaxy (i.e. the time elapsed since it assembled most of its current stellar mass) may not coincide with the age of its underlying stellar population. As a consequence the processes of star formation and mass assembly remain distinct: it is possible that stars which formed long ago were assembled only recently in a newly created galaxy (Renzini 2007; Cimatti et al. 2006; Bundy et al. 2006).

Within such a scenario one considers two separate downsizing signatures, i.e. downsizing in star formation (the transfer of star formation activity to lower mass galaxies) and downsizing in mass assembly (irrespectively by type classification, massive galaxies are fully assembled at early times, with less massive galaxies assembling later). If one or more mechanisms are responsible for quenching star formation activity earlier in massive galaxies, and if dry mergers represent only a minor contribution to the galaxy mass assembly, then the two concepts of downsizing express one single idea. In the previous sections we have found that the distribution of the stellar ages and stellar mass can be interpreted in the framework of a top-down picture of the stellar mass assembly history of galaxies. However, we made no hypothesis on the mechanism or mechanisms that lead the stellar mass to aggregate, leaving open the possibility of mass accretion by both merging and star formation activity.

Can the galaxy star formation rates and their efficiencies alone justify the observed mass assembly history without invoking any (dry) merger mechanism? To investigate this issue we define for each galaxy at redshift z the time Δt as the time interval between the age of the Universe at the observed redshift z and the time corresponding to the lower limit of the redshift bin in which the galaxy falls. For three redshift bins in Fig. 5 we plot with left-leaning diagonals (blue-coded) the D_n4000 distribution of galaxies which assemble enough stellar mass to move to a higher mass interval only on the basis of their estimated SFRs within a time Δt. The assumption is that galaxies will sustain a SFR, equal to the observed one, over the time Δt. This appears to be a reasonable assumption as our Δt is never larger than 1.3 Gyr. The right-leaning diagonals (red-coded) represent the galaxies which, given their observed SFR, would remain over the time Δt in the mass interval assigned at the time of the observations.

Figure 5 shows that the lower the stellar mass the larger is the fraction of galaxies which sustain a significant stellar mass growth, i.e. not only forming stars as a local and episodic event but also effectively assembling mass. Once a galaxy reaches a certain stellar mass, it terminates to grow efficiently. The physical reason could be the natural exhaustion of the gas reservoir contained in massive galaxies which did consume it efficiently in the first phase of their life. On the contrary, low-mass galaxies, having sustained a lower rate of star formation activity over the time still have a certain amount of fueling.

The fraction of galaxies that increase significantly their stellar mass (blue-coded population) is larger than the fraction of galaxies that is not effectively assembling mass (red-coded) at lower stellar masses with time. The evolution of the characteristic stellar mass at which blue- and red-coded populations are equally contributing to the total population parallels that of the quenching mass, defined as the mass at which no active systems are observed (see for details Bundy et al. 2006).

For each stellar mass bin Fig. 5 shows a decline in the mass assembly efficiency from high to low redshifts. Similarly for each redshift bin there is a decline in the mass assembly efficiency moving from low to high stellar masses. Interestingly, the few massive galaxies which can still potentially increase their mass are classified as late-types from D_n4000.

These results and those obtained in previous sections support the hypothesis of apparent no evolution in the blue sequence proposed by Faber et al. (2007) and the mild evolution of the early-type class of galaxies (Zucca et al. 2006; Brown et al. 2007; Arnouts et al. 2007) which are largely inefficient at assembling mass at all epochs (at least since $z \sim 1.3$), and are progressively decreasing their efficiency as cosmic time progresses. In particular, on the basis of the mass migration from blue to red objects, Arnouts et al. (2007) propose a similar time-scale for the period required for blue galaxies to quench their star formation activity and move to the red sequence, and the birth rate time of blue galaxies which are continuously refilled by new stars.

If we consider the galaxies with stellar mass M_i ($\log(M/M_\odot)_{i=1,2,3,4,5} = 9-9.5, 9.5-10, 10-10.5, 10.5-11, >11$) observed at redshift z_j ($z_{j=1,2,3} = 0.5-0.7, 0.7-1, 1-1.3$), their progenitors are the sum of two galaxy contributions if no merging activity is advocated. The first progenitor class is constituted by galaxies with mass M_{i-1} at z_{j-1} that are assembling enough stellar mass to migrate in the higher mass interval within a time Δt, where Δt was previously defined (e.g. blue-coded galaxies at $z = 0.7-1$ and $\log(M) = 10.5-11 \, M_\odot$). The second contributors are galaxies with stellar mass included in the same mass interval (M_i) at the epoch z_{j-1} that in a time Δt are not growing
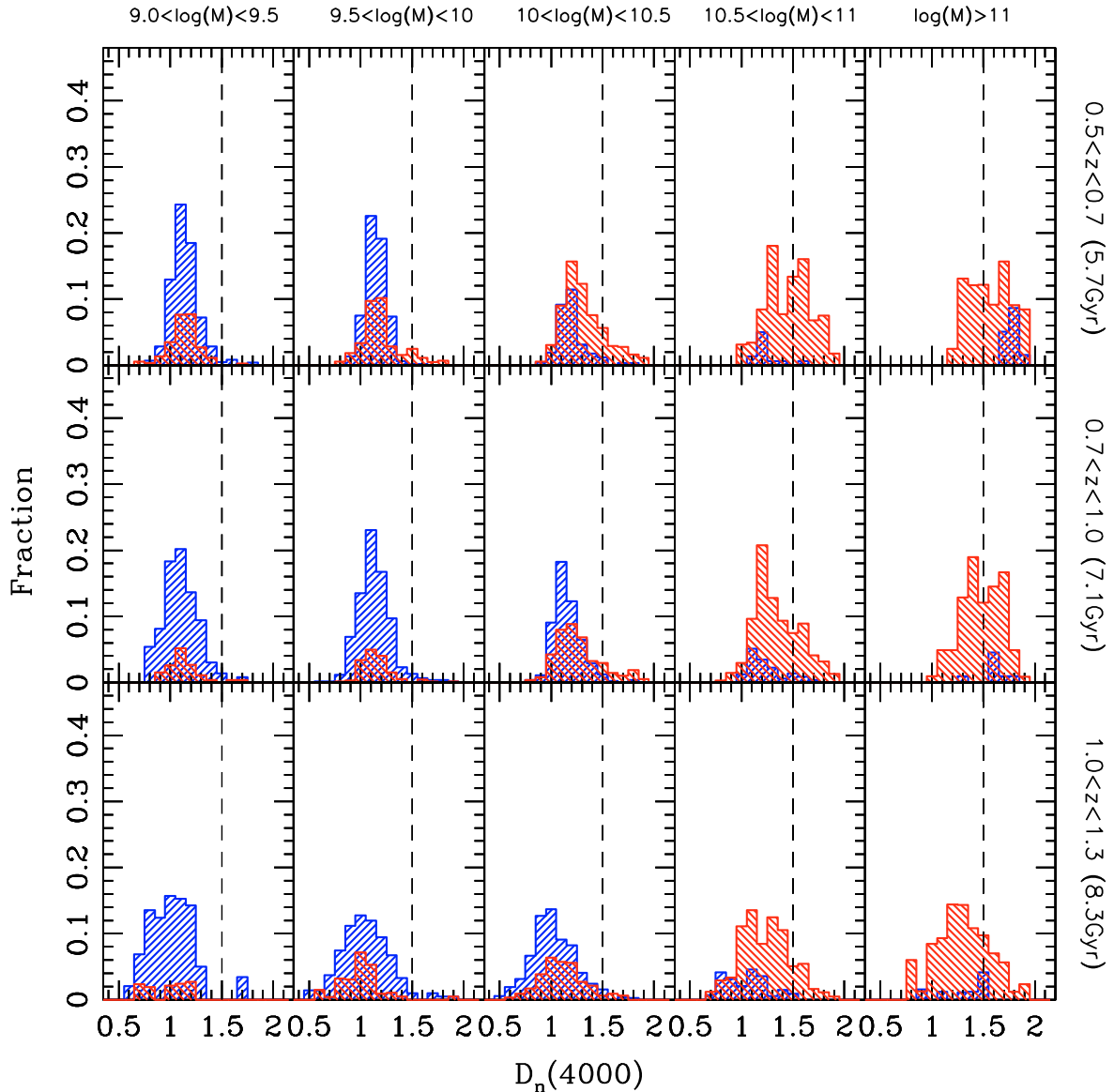
Fig. 5. Histograms showing the fraction of VVDS galaxies as a function of D_n4000 for five different ranges of stellar mass at three redshift epochs $(0.5-0.7, 0.7-1.0, 1.0-1.3)$. The corresponding look-back time is also indicated. We define Δt for each galaxy at redshift z as the time interval between the age of the Universe at the observed redshift z and the time corresponding to the lower limit of the redshift bin in which the galaxy falls. Left-leaning diagonal (blue) histograms represent those galaxies that assemble within a time Δt a stellar mass enough to move to a higher mass interval and with right-leaning diagonals (red) those staying in the mass interval assigned at the time of the observations. The assumption is that these galaxies will sustain a constant observed SFR over the time Δt, which turns to be a reasonable assumption as our Δt is never larger than 1.3 Gyr.

sufficient mass to flow in the subsequent stellar mass interval (e.g. red-coded galaxies at $z = 0.5-0.7$ and $\log(M) > 11\ M_\odot$).

We compute within our mass completeness limit the number (per unit of co-moving volume) of galaxies observed at redshift z_j of stellar mass M_i and that of progenitors at redshift z_{j-1} as described above. We obtain that the number of progenitors at z_{j-1} defined as above can account, on average, for $(80 \pm 10)\%$ of the galaxies at z_j of stellar mass M_i, and therefore that no significant contribution to the mass assembly process is required from merging activity. The agreement between number of progenitors and number of observed galaxies improves moving to higher masses, reaching nearly 100% for $\log(M) > 10.5\ M_\odot$. This result shows that star formation activity alone can explain the observed evolution of stellar mass function up to $z \sim 1$. A similar conclusion has been presented recently by Bundy et al. (2007)

for spheroidal galaxies comparing the dynamical and stellar mass in the GOODS fields. The match between the growth rate in the abundance of spheroidals with that predicted by the assembly of dark matter halos enables Bundy et al. to state that merging is not the primary mechanism to form spheroids and additional mechanisms as morphological transformations are required to drive the observed evolution. Further convincing evidence that a significant number of massive blue galaxies must have quenched their star formation and moved to the red sequence without invoking any merging mechanism is provided by e.g. Scarlata et al. (2007) and Bell et al. (2007). This picture satisfies both the luminosity and mass function constraints.

The scenario described here, if correct, implies that all recent observations on galaxy evolution can be summarised with one single concept of downsizing, as downsizing in star formation

and downsizing in mass assembly go in parallel. Still, a more detailed and quantitative analysis of the mass function and star formation rate evolution are needed before a more accurate evaluation of the role played by mergers in the build up of the galaxy mass can be obtained. It is in fact well known that mergers do take place and recently individual cases of dry mergers have also been listed by e.g. Bell et al. (2006) and Tran et al. (2005). We cannot therefore exclude the possibility that between two redshift bins a small fraction of galaxies moves from mass bin M_i to a higher mass bin via merger.

A possible objection to the scenario in which merging would not be important is the large fraction of galaxies up to $z = 1$ possessing spatial and kinematic asymmetries (e.g. Flores et al. 2006; Puech et al. 2007). These lopsided galaxies are very often associated to merging of galaxies. However there exist various ranges of mass merging fractions and several mechanisms (slow accretion, gravitational interaction, etc.) that can justify the observed asymmetric properties and are not probed by the current surveys. It could very well be that major mergers – that are those that we are constraining with our analysis – are not needed to explain the observed lopsidedness frequency. These surely are issues to investigate with future (gas multi-phase) surveys.

5. Summary

We have investigated the relationship between galaxy stellar age and stellar mass as a function of redshift in a mass-complete spectroscopic sample selected from the VIMOS VLT Deep Survey (VVDS). Up to $z \sim 1.3$ we confirmed the presence of a relationship mass-stellar ages that parallels the one observed in the local Universe (see Kauffman et al. 2003b). In all redshift bins explored, low-mass galaxies ($\log(M) < 10\ M_\odot$) are dominated by a young stellar population, as witnessed by the low D_n4000 values. For higher mass galaxies ($\log(M) > 10\ M_\odot$), the percentage of galaxies dominated by an old stellar population is much higher and grows regularly with cosmic time. This process is more efficient the higher the galaxy stellar mass considered. This result supports the so-called "assembly downsizing": the stellar population in massive galaxies formed at earlier times than the one in low-mass galaxies.

We then explored SFR evolution as a function of stellar mass. The percentage of quiescent galaxies, as witnessed by their low EW[OII] values, increases when moving to lower redshifts and higher masses. This trend is clearly visible both for galaxies with a young stellar population and for galaxies with an old stellar population. The emerging picture is one where low-mass galaxies ($\log(M) < 10\ M_\odot$) are subject to bursts of star formation activity up to recent times, while the dominant mode of star formation for massive galaxies ($\log(M) > 10\ M_\odot$) is a smooth one, with no significant contributions from secondary strong bursts. Therefore not only does the bulk of the stellar population in massive galaxies form at earlier times but the location where the mass also gets assembled more efficiently at each redshift moves to lower mass galaxies with cosmic time.

We have also shown a mild total evolution with redshift of mass assembly history, in particular for the very massive galaxies ($\log(M) > 11.4\ M_\odot$) which are mainly early-type objects, up to the highest sample redshift ($z \sim 1.3$). Since the relative fraction of massive ($\log(M) > 10.5\ M_\odot$) early- and late-type galaxies evolves with cosmic time, we are witnessing a spectral transformation of late-type systems into old massive galaxies at lower redshift.

Finally, when we consider the joint distribution of stellar mass and star formation activity to quantify the efficiency with which galaxies assemble their stellar mass, we obtain a scenario where it is possible to account for the number of passively evolving galaxies up to $z \sim 1$ without invoking any (dry) merging mechanism. Our observations agree well with a scenario where the stellar population in massive galaxies formed earlier than the one in low-mass galaxies, and massive galaxies themselves were the first to be assembled.

References

Adelman-McCarthy, J. K., Agüeros, M. A., Allam, S. S., et al. 2006, ApJS, 162, 38
Arnouts, S., Walcher, C. J., Le Fèvre, O., et al. 2007, A&A, 476, 137
Baldry, I. K., Glazebrook, K., Brinkmann, J., et al. 2004, ApJ, 600, 681
Balogh, M. L., Morris, S. L., Yee, H. K. C., Carlberg, R. G., & Ellingson, E. 1999, ApJ, 527, 54
Bauer, A. E., Drory, N., Hill, G. J., & Feulner, G. 2005, ApJ, 621, L89
Bell, E. F., Naab, T., McIntosh, D. H., et al. 2006, ApJ, 640, 241
Bell, E. F., Zheng, X. Z., Papovich, C., et al. 2007, ApJ, 663, 834
Borch, A., Meisenheimer, K., Bell, E. F., et al. 2006, A&A, 453, 869
Bottini, D., Garilli, B., Maccagni, D., et al. 2005, PASP, 117, 996
Bower, R. G., Benson, A. J., Malbon, R., et al. 2006, MNRAS, 370, 645
Brinchmann, J., & Ellis, R. S. 2000, ApJ, 536, L77
Brown, M. J. I., Dey, A., Jannuzi, B. T., et al. 2007, ApJ, 654, 858
Bruzual, G. 1983, ApJ, 273, 105
Bruzual, G., & Charlot, S. 2003, MNRAS, 344, 1000
Bundy, K., Ellis, R. S., & Conselice, C. J. 2005, ApJ, 625, 621
Bundy, K., Ellis, R. S., Conselice, C. J., et al. 2006, ApJ, 651, 120
Bundy, K., Treu, T., & Ellis, R. S. 2007, ArXiv e-prints, 705
Charlot, S., & Longhetti, M. 2001, MNRAS, 323, 887
Cimatti, A., Daddi, E., Mignoli, M., et al. 2002, A&A, 381, L68
Cimatti, A., Daddi, E., Renzini, A., et al. 2004, Nature, 430, 184
Cimatti, A., Daddi, E., & Renzini, A. 2006, A&A, 453, L29
Cowie, L. L., Songaila, A., Hu, E. M., & Cohen, J. G. 1996, AJ, 112, 839
Cucciati, O., Iovino, A., Marinoni, C., et al. 2006, A&A, 458, 39
De Lucia, G., Springel, V., White, S. D. M., Croton, D., & Kauffmann, G. 2006, MNRAS, 366, 499
Faber, S. M., Willmer, C. N. A., Wolf, C., et al. 2007, ApJ, 665, 265
Felten, J. E. 1976, ApJ, 207, 700
Feulner, G., Gabasch, A., Salvato, M., et al. 2005a, ApJ, 633, L9
Feulner, G., Goranova, Y., Drory, N., Hopp, U., & Bender, R. 2005b, MNRAS, 358, L1
Fioc, M., & Rocca-Volmerange, B. 1997, A&A, 326, 950
Flores, H., Hammer, F., Puech, M., Amram, P., & Balkowski, C. 2006, A&A, 455, 107
Fontana, A., Pozzetti, L., Donnarumma, I., et al. 2004, A&A, 424, 23
Förster Schreiber, N. M., Genzel, R., Lehnert, M. D., et al. 2006, ApJ, 645, 1062
Franzetti, P. 2005, Ph.D. Thesis, University of Milano Bicocca
Franzetti, P., Scodeggio, M., Garilli, B., et al. 2007, A&A, 465, 711
Gallazzi, A., Charlot, S., Brinchmann, J., White, S. D. M., & Tremonti, C. A. 2005, MNRAS, 362, 41
Gavazzi, G., Bonfanti, C., Sanvito, G., Boselli, A., & Scodeggio, M. 2002, ApJ, 576, 135
Genzel, R., Tacconi, L. J., Eisenhauer, F., et al. 2006, Nature, 442, 786
Giavalisco, M., Ferguson, H. C., Koekemoer, A. M., et al. 2004, ApJ, 600, L93

Guzman, R., Gallego, J., Koo, D. C., et al. 1997, ApJ, 489, 559
Hamilton, D. 1985, ApJ, 297, 371
Heavens, A., Panter, B., Jimenez, R., & Dunlop, J. 2004, Nature, 428, 625
Hopkins, A. M., & Beacom, J. F. 2006, ApJ, 651, 142
Ilbert, O., Tresse, L., Zucca, E., et al. 2005, A&A, 439, 863
Iovino, A., McCracken, H. J., Garilli, B., et al. 2005, A&A, 442, 423
Jimenez, R., Panter, B., Heavens, A. F., & Verde, L. 2005, MNRAS, 356, 495
Juneau, S., Glazebrook, K., Crampton, D., et al. 2005, ApJ, 619, L135
Kauffmann, G., Heckman, T. M., White, S. D. M., et al. 2003a, MNRAS, 341, 33
Kauffmann, G., Heckman, T. M., White, S. D. M., et al. 2003b, MNRAS, 341, 54
Kauffmann, G., Heckman, T. M., De Lucia, G., et al. 2006, MNRAS, 367, 1394
Kennicutt, R. C. 1989, ApJ, 344, 685
Kodama, T., Yamada, T., Akiyama, M., et al. 2004, MNRAS, 350, 1005
Kriek, M., van Dokkum, P. G., Franx, M., et al. 2006, ApJ, 645, 44
Labbé, I., Rudnick, G., Franx, M., et al. 2003, ApJ, 591, L95
Lamareille, F., Contini, T., Brinchmann, J., et al. 2006, A&A, 448, 907
Lawrence, A., Warren, S. J., Almaini, O., et al. 2007, MNRAS, 379, 1599
Le Borgne, D., Abraham, R., Daniel, K., et al. 2006, ApJ, 642, 48
Le Fèvre, O., Mellier, Y., McCracken, H. J., et al. 2004a, A&A, 417, 839
Le Fèvre, O., Vettolani, G., Paltani, S., et al. 2004b, A&A, 428, 1043
Le Fèvre, O., Vettolani, G., Garilli, B., et al. 2005, A&A, 439, 845
Lilly, S. J., Le Fevre, O., Hammer, F., & Crampton, D. 1996, ApJ, 460, L1
Lonsdale, C. J., Smith, H. E., Rowan-Robinson, M., et al. 2003, PASP, 115, 897
Madau, P., Ferguson, H. C., Dickinson, M. E., et al. 1996, MNRAS, 283, 1388
Martin, D. C., Wyder, T. K., Schiminovich, D., et al. 2007, ArXiv Astrophysics e-prints
McCarthy, P. J., Le Borgne, D., Crampton, D., et al. 2004, ApJ, 614, L9
McCracken, H. J., Radovich, M., Bertin, E., et al. 2003, A&A, 410, 17
McCracken, H. J., Ilbert, O., Mellier, Y., et al. 2007, ArXiv e-prints, 711
Meneux, B., Le Fèvre, O., Guzzo, L., et al. 2006, A&A, 452, 387
Mignoli, M., Cimatti, A., Zamorani, G., et al. 2005, A&A, 437, 883
Miller, N. A., & Owen, F. N. 2002, AJ, 124, 2453
Mouhcine, M., Lewis, I., Jones, B., et al. 2005, MNRAS, 362, 1143
Neistein, E., van den Bosch, F. C., & Dekel, A. 2006, MNRAS, 372, 933
Noeske, K. G., Faber, S. M., Weiner, B. J., et al. 2007, ArXiv Astrophysics e-prints
Peebles, P. J. E. 1980, The large-scale structure of the universe (Princeton University Press), 435
Pozzetti, L., Bolzonella, M., Lamareille, F., et al. 2007, A&A, 474, 443
Puech, M., Hammer, F., Flores, H., et al. 2007, A&A, 476, L21
Radovich, M., Arnaboldi, M., Ripepi, V., et al. 2004, A&A, 417, 51
Renzini, A. 2006, ARA&A, 44, 141
Renzini, A. 2007, ArXiv Astrophysics e-prints
Salpeter, E. E. 1955, ApJ, 121, 161
Savaglio, S., Glazebrook, K., Le Borgne, D., et al. 2005, ApJ, 635, 260
Scarlata, C., Carollo, C. M., Lilly, S. J., et al. 2007, ApJS, 172, 494
Schmidt, M. 1968, ApJ, 151, 393
Scodeggio, M., Franzetti, P., Garilli, B., et al. 2005, PASP, 117, 1284
Somerville, R. S., Lee, K., Ferguson, H. C., et al. 2004, ApJ, 600, L171
Stockton, A., Canalizo, G., & Maihara, T. 2004, ApJ, 605, 37
Strateva, I., Ivezić, Ž., Knapp, G. R., et al. 2001, AJ, 122, 1861
Temporin, S., Iovino, A., McCracken, H. J., et al. 2006, ArXiv Astrophysics e-prints
Thomas, D., Maraston, C., Bender, R., & Mendes de Oliveira, C. 2005, ApJ, 621, 673

Tran, K.-V. H., van Dokkum, P., Franx, M., et al. 2005, ApJ, 627, L25
Tremonti, C. A., Heckman, T. M., Kauffmann, G., et al. 2004, ApJ, 613, 898
Tresse, L., Ilbert, O., Zucca, E., et al. 2006, ArXiv Astrophysics e-prints
Weiner, B. J., Papovich, C., Bundy, K., et al. 2007, ApJ, 660, L39
Zanichelli, A., Garilli, B., Scodeggio, M., et al. 2005, PASP, 117, 1271
Zheng, X. Z., Bell, E. F., Papovich, C., et al. 2007, ApJ, 661, L41
Zucca, E., Ilbert, O., Bardelli, S., et al. 2006, A&A, 455, 879

[1] IASF – INAF, via Bassini 15, 20133, Milano, Italy
e-mail: daniela@lambrate.inaf.it
[2] INAF – Osservatorio Astronomico di Bologna, via Ranzani 1, 40127, Bologna, Italy
[3] INAF – Osservatorio Astronomico di Brera, via Brera 28, 20021, Milan, Italy
[4] Laboratoire d'Astrophysique de Marseille, UMR 6110 CNRS-Université de Provence, BP 8, 13376 Marseille Cedex 12, France
[5] Max-Planck-Institut für Astrophysik, 85741, Garching, Germany
[6] Institut d'Astrophysique de Paris, UMR 7095, 98bis Bvd Arago, 75014 Paris, France
[7] Laboratoire d'Astrophysique de Toulouse/Tarbes (UMR 5572), CNRS, Université Paul Sabatier – Toulouse III, Observatoire Midi-Pyrénées, 14 Av. E. Belin, 31400 Toulouse, France
[8] IRA – INAF, via Gobetti, 101, 40129 Bologna, Italy
[9] INAF – Osservatorio Astronomico di Roma, via di Frascati 33, 00040 Monte Porzio Catone, Italy
[10] School of Physics & Astronomy, University of Nottingham, University Park, Nottingham, NG72RD, UK
[11] Astrophysical Institute Potsdam, An der Sternwarte 16, 14482 Potsdam, Germany
[12] Institute for Astronomy, 2680 Woodlawn Dr., University of Hawaii, Honolulu, Hawaii, 96822, USA
[13] Observatoire de Paris, LERMA, 61 avenue de l'Observatoire, 75014 Paris, France
[14] Università di Bologna, Dipartimento di Astronomia, via Ranzani 1, 40127 Bologna, Italy
[15] Centre de Physique Théorique, UMR 6207 CNRS-Université de Provence, 13288 Marseille, France
[16] Integral Science Data Centre, Ch. d'Écogia 16, 1290 Versoix, Switzerland
[17] Geneva Observatory, Ch. des Maillettes 51, 1290 Sauverny, Switzerland
[18] Astronomical Observatory of the Jagiellonian University, ul Orla 171, 30-244 Kraków, Poland
[19] INAF – Osservatorio Astronomico di Capodimonte, via Moiariello 16, 80131 Napoli, Italy
[20] Centro de Astrofísica da Universidade do Porto, Rua das Estrelas, 4150-762 Porto, Portugal
[21] Università di Milano-Bicocca, Dipartimento di Fisica, Piazza delle Scienze 3, 20126 Milano, Italy
[22] Laboratoire AIM, CEA/DSM – CNRS – Université Paris Diderot, IRFU/SAp, 91191 Gif-sur-Yvette, France